

# Search for First-Generation Scalar Leptoquarks in $p\bar{p}$ collisions at $\sqrt{s}=1.96$ TeV

(Dated: March 7, 2005)

We report on a search for pair production of first-generation scalar leptoquarks ( $LQ$ ) in  $p\bar{p}$  collisions at  $\sqrt{s}=1.96$  TeV using an integrated luminosity of  $203\text{ pb}^{-1}$  collected at the Fermilab Tevatron collider by the CDF detector. We observe no evidence for  $LQ$  production in the topologies arising from  $LQ\bar{L}Q \rightarrow e\bar{e}q\bar{q}$  and  $LQ\bar{L}Q \rightarrow e\nu q\bar{q}$ , and derive 95% C.L. upper limits on the  $LQ$  production cross section as a function of  $\beta$ , where  $\beta$  is the branching fraction for  $LQ \rightarrow e\bar{q}$ . The results are combined with those obtained from a CDF search in the topology arising from  $LQ\bar{L}Q \rightarrow \nu q \nu \bar{q}$  and 95% C.L. lower limits on the  $LQ$  mass as a function of  $\beta$  are derived. The limits are 236, 205 and 145 GeV/c<sup>2</sup> for  $\beta = 1$ ,  $\beta = 0.5$  and  $\beta = 0.1$ , respectively.

PACS numbers:

The remarkable symmetry between quarks and leptons in the Standard Model (SM) suggests that some more fundamental theory may exist, which could allow for interactions between them. Such interactions could be mediated by a new type of particle, the leptoquark,  $LQ$ [1], which carries both lepton and baryon number, is a color triplet boson with spin 0 or 1, and has fractional charge. Leptoquarks are predicted in many extensions of the SM (e.g. grand unification, technicolor, and supersymmetry with R-parity violation[2]). Usually it is assumed that leptoquarks couple to fermions of the same generation to accommodate experimental constraints on flavor changing neutral currents and helicity suppressed decays. This allows one to classify leptoquarks as first-, second-, or third-generation. Previous limits on leptoquark production from Tevatron Run I, HERA and LEP, are summarized in [3]. The H1 and ZEUS experiments at the  $e^\pm p$  collider HERA at DESY published[4] lower limits on the mass of a first generation  $LQ$  that depend on the unknown leptoquark  $l-q$  Yukawa coupling  $\lambda$ . At the CERN LEP collider, pair production of first generation leptoquarks can occur in  $e^+e^-$  collisions via a virtual  $\gamma$  or  $Z$  boson in the  $s$ -channel. At the Fermilab Tevatron collider, leptoquarks would be pair produced predominantly through  $q\bar{q}$  annihilation (for  $M_{LQ} > 100\text{ GeV}/c^2$ ) and gluon fusion. Such pair production mechanisms are independent of the coupling  $\lambda$ . Experiments at the LEP collider [5] and at the Fermilab Tevatron[6–8] have set lower limits on the masses of leptoquarks. In this Letter, we present a search for first-generation scalar leptoquark pairs produced in  $p\bar{p}$  collisions at  $\sqrt{s}=1.96$  TeV for two cases: when both leptoquarks decay to an electron and a quark with a branching fraction (Br)  $\beta^2$  where  $\beta$  is the leptoquark branching fraction into an electron and a quark and when one of the leptoquarks decays to an electron and a quark and the other to a neutrino and a quark with  $\text{Br} = 2\beta(1 - \beta)$ . The final states consist of two electrons and two jets ( $eejj$ ) or of an electron, two jets, and missing transverse energy corresponding to the neutrino which escapes detection ( $e\nu jj$ ). These results are then combined with those from a search for scalar leptoquark pairs decaying into  $\nu\nu q\bar{q}$ , resulting in a jets and missing transverse energy topology[8].

CDF is a general-purpose detector built to study the physics of  $p\bar{p}$  collisions at the Tevatron accelerator at Fermilab. The main components are a silicon vertex detector, central tracking drift chamber, central and forward calorimeters, and muon chambers. The detector is described in detail elsewhere [9]. The data used in the analysis were collected during the 2002-2003 Tevatron Run II. The integrated luminosity for this data sample is  $203 \pm 12.2\text{ pb}^{-1}$ . Events were required to pass the high  $P_T$  electron triggers, based on the requirement of one electromagnetic trigger tower to be above threshold and a set of identification cuts on the electromagnetic cluster, track and shower profile. The efficiency of the trigger combinations used in the  $eejj$  and  $e\nu jj$  analyses have been measured using data. They are  $\sim 100\%$  for two electrons with transverse energy  $E_T > 25\text{ GeV}/c$ . The trigger efficiency for one single electron with  $E_T > 25\text{ GeV}/c$  is  $\sim 96\%$ . Electrons are reconstructed offline as calorimeter electromagnetic clusters matching a track in the central-tracking system (central electrons,  $|\eta| < 1.1$ [10]) or as calorimeter electromagnetic clusters only in the forward region ( $|\eta| \leq 3$ ). Electromagnetic clusters are identified by the characteristics of their energy deposition in the calorimeter: cuts are applied on the fraction of the energy in the electromagnetic calorimeter and the isolation of the cluster. Identification efficiency for a pair of central electrons is  $\sim 92\%$  and for a pair of central-forward electrons  $\sim 80\%$ . The coordinate of the lepton (also assumed to be the event coordinate) along the beamline must fall within 60 cm of the center of the detector ( $z_{\text{vertex}}$  cut) to ensure a good energy measurement in the calorimeter. This cut is 95% efficient, from studies with minimum bias events. The efficiencies of the identification cuts, the trigger selection and the vertex cut, measured using the data were taken into account using proper weightings of the MC events. Jets are reconstructed using a cone of fixed radius  $\Delta R = 0.7$  in the  $\eta - \phi$  plane. They are required to have  $|\eta| < 2.0$ . The energy measurement of the jets has been calibrated as a function of the jet transverse energy and  $\eta$  by balancing energy in the photon plus jets events. Neutrinos produce missing transverse energy,  $\cancel{E}_T$ , which is measured by balancing the calorimeter energy in the transverse plane.

In the dielectron and jets topology, from the inclusive electron triggers dataset we select events with two reconstructed isolated electrons with  $E_T > 25$  GeV/c. The first electron is required to be central, while the second can be central or forward. Events are further selected if there are at least two jets with  $E_T > 30$  and 15 GeV/c. The dataset selected above is dominated by QCD production of  $Z$  bosons in association with jets and  $t\bar{t}$  production (where both the  $W$ 's from top decay into an electron and neutrino). To reduce these backgrounds the following cuts are applied: i) veto of events whose reconstructed dilepton mass falls in the window  $76 < m_{ee} < 110$  GeV/c<sup>2</sup> to remove the  $Z$  + jets contribution, ii)  $E_T(j_1) + E_T(j_2) > 85$  GeV/c and  $E_T(e_1) + E_T(e_2) > 85$  GeV/c, iii)  $\sqrt{((E_T(j_1) + E_T(j_2))^2 + (E_T(e_1) + E_T(e_2))^2)} > 200$  GeV/c. We studied the properties of the  $Z$  + jets and top backgrounds by generating the process  $Z + 2$  jets with Alpgen[11] and  $t\bar{t}$  with PYTHIA[12] and passing them through a complete simulation of the CDF II detector based on GEANT[13] and complete event reconstruction. Other backgrounds from  $b\bar{b}$ ,  $Z \rightarrow \tau\bar{\tau}$ ,  $WW$  are negligible due to the electron isolation and large electron and jet transverse energy requirements. To normalize simulated events to data we used the theoretical cross sections for  $t\bar{t}$  from [14] and for  $\gamma/Z \rightarrow ee + 2$  jets from [15]. The expected number of  $Z + 2$  jets events is  $1.89 \pm 0.44$ . The expected number of  $t\bar{t}$  events is  $0.35 \pm 0.03$  events. The total number of expected physics background events is  $2.24 \pm 0.44$ . The background arising from multijet events where a jet is mismeasured as an electron (fake) is calculated using data, for both this analysis and the one that follows. The method used relies on the assumption that since jets are produced in association with other particles, the isolation fraction of a jet will be generally larger than the one corresponding to an electron. The isolation fraction is defined here as:  $E_T^{cone} - E_T^{cluster} / E_T^{cluster}$  where  $E_T^{cone}$  is the sum of the electromagnetic and transverse energies measured in all towers in a radius  $R = \sqrt{(\Delta\phi^2 + \Delta\eta^2)}$  around the electron and  $E_T^{cluster}$  is the transverse electromagnetic energy of the electron. The phase space corresponding to the two electrons isolation fractions ( $eejj$ ) or to one electron isolation fraction and the  $\cancel{E}_T$  ( $evjj$ ) is divided in different regions. The following assumptions are made: there is no correlation between the isolation of the two electrons ( $eejj$ ) and the isolation of the electron and  $\cancel{E}_T$  ( $evjj$ ); and in the region where both electrons have large isolation fraction ( $eejj$ ), or where the  $\cancel{E}_T$  is small and the isolation fraction of the electron is large ( $evjj$ ) the  $LQ$  contribution is expected to be negligible. We will call these background-dominated regions. With these assumptions, from the ratio of the number of events in the background-dominated regions we can extrapolate the contribution in the signal region. We estimate  $0_{-0}^{+0.7}$  fake events in the central-central category and  $3.96 \pm 1.98$  in the central-forward category. The final background estimate is  $6.24 \pm 2.16$  events. We checked the prediction

TABLE I: Efficiencies after all cuts, relative errors and 95% C.L. upper limits on the production cross section  $\times$  branching fraction Br, as a function of  $M_{LQ}$ , for the two channels.

$M_{LQ}(\text{GeV}/c^2)$	$eejj$		$evjj$	
	$\epsilon$	$\sigma \times \text{Br}(\text{pb})$	$\epsilon$	$\sigma \times \text{Br}(\text{pb})$
100	$0.07 \pm 0.07$	1.11	$0.02 \pm 0.13$	5.71
140	$0.12 \pm 0.04$	0.25	$0.08 \pm 0.09$	0.69
160	$0.21 \pm 0.04$	0.14	$0.08 \pm 0.09$	0.65
200	$0.32 \pm 0.05$	0.09	$0.16 \pm 0.08$	0.37
220	$0.35 \pm 0.05$	0.08	$0.19 \pm 0.08$	0.24
240	$0.38 \pm 0.04$	0.07	$0.20 \pm 0.08$	0.23
260	$0.40 \pm 0.04$	0.07	$0.22 \pm 0.08$	0.22

of our background sources with data in a control region defined by requiring two electrons with  $E_T > 25$  GeV/c, 2 jets with  $E_T > 30$  GeV/c and  $66 < m_{ee} < 110$  GeV/c<sup>2</sup>. We observe 107 events in agreement with  $113 \pm 15$  predicted from SM processes. The efficiency to detect our signal was obtained from MC simulated LQ (PYTHIA) to account for kinematical and geometrical acceptances. The total efficiencies for a LQ signal are reported in Table I. The following systematic uncertainties are considered when calculating signal acceptance and background predictions: i) luminosity: 6% ii) choice of parton distribution functions: 2.1% iii) statistical uncertainty of MC < 1% iv) jet energy scale < 1% v) statistics of  $Z \rightarrow e^+e^-$  sample: 0.8% vi)  $z_{vertex}$  cut: 0.5%. After all selection cuts, 4 events are left in our data.

In the search in the electron, neutrino and two jets topology, from the inclusive lepton dataset we select events offline with one reconstructed isolated electron with  $E_T > 25$  GeV/c. The electron is required to be central ( $|\eta| \leq 1$ ). We veto events with a second central or forward electron to be orthogonal to the previous analysis. We then select events where there is large missing transverse energy,  $\cancel{E}_T > 60$  GeV/c and at least two jets with  $E_T > 30$  GeV/c in the range  $|\eta| \leq 2$ . The dataset selected is dominated by QCD production of  $W$  bosons in association with jets and top quark where either both the  $W$ 's from the top pair decay into  $\nu\bar{\nu}$  and one lepton is mismeasured, or one of the  $W$  decays leptonically and the other hadronically. A small source of background is represented by  $Z + 2$  jets, where one of the electrons is not identified. To reduce these backgrounds the following cuts are applied: i)  $\Delta\phi(\cancel{E}_T - jet) > 10^\circ$  to veto events where the transverse missing energy is mis-measured due to a mismeasured jet, ii)  $E_T(j_1) + E_T(j_2) > 80$  GeV/c, iii)  $M_T(\nu\bar{\nu}) > 120$  GeV/c<sup>2</sup> to reduce the  $W + 2$  jets contribution. We studied the properties of the  $W + 2$  jets,  $t\bar{t}$  and  $Z + 2$  jets backgrounds as described above. The background from  $W \rightarrow \nu\tau + 2$  jets (Alpgen) is negligible after the final window mass cut (see below), as well as the QCD fakes background (described above). Our final cut consists in selecting events falling in mass windows defined around several LQ masses. The mass window

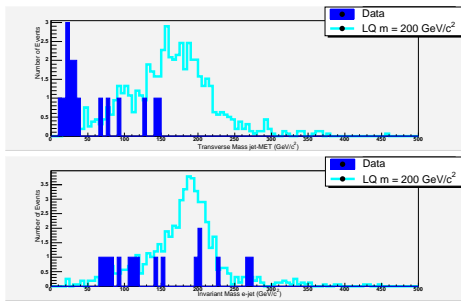


FIG. 1: Fig 1: Final mass distribution of the surviving events (before the mass limit cut) compared to the signal distribution for  $M_{LQ} = 200 \text{ GeV}/c^2$

is built as follows. We calculate the invariant mass of the electron-jet system and the transverse mass of the neutrino-jet system. Given the decay of the two LQ's, there are two possible mass combinations for the electron and the neutrino with the two leading jets. We choose the combinations that minimize the difference between the electron-jet mass and the neutrino-jet transverse mass. We fit the peak of the  $e$ -jet distribution with a Gaussian, to obtain an estimate of the spread of the distribution in the signal region ( $\sigma_e$ ), as well as the  $\nu$ -jet transverse mass distribution, taking into account its high tail, to obtain  $\sigma_\nu$ . In the kinematic plane of  $m(e-jet)$  vs  $m_T(\nu-jet)$  we define the sides of rectangular boxes centered around various nominal LQ mass as  $3 \times \sigma_{e,\nu}$ . For each LQ mass, events are accepted if they fall inside the rectangular box. The total efficiency of these cuts for several LQ masses is given in Table I. In Fig. 1 we plot the final mass distribution of the selected events (before the mass limit cut) compared to the signal distribution for  $m_{LQ} = 200 \text{ GeV}/c^2$ . We checked the simulation prediction of our background sources with data in a control region defined by requiring one electron with  $E_T > 25 \text{ GeV}/c$ ,  $\cancel{E}_T > 35 \text{ GeV}/c$  and 2 jets with  $E_T > 30 \text{ GeV}/c$ . We observe 536 events in agreement with  $503 \pm 22$  predicted from SM processes. The number of events in each mass region, compared with the background expectations is reported in Table II. The efficiency to detect our signal was obtained from MC simulated LQ data (PYTHIA) as described above. The following systematic uncertainties are considered when calculating signal acceptance and background predictions: i) luminosity: 6% ii) choice of the parton distribution functions: 2.1% iii) statistics of MC < 1.0% ; iv) jet energy scale < 1% v) electron identification 0.6% vi)  $z_{vertex}$  cut: 0.5% vii) initial and final state radiation: 1.7%.

In the analyses described above the number of events passing the selection cuts is consistent with the expected number of background events. The conclusion of the two searches is that there is no LQ signal: we derive an upper limit on the leptoquark production cross section at 95% We use a Bayesian approach[16] with a flat prior for the sig-

TABLE II: Final number of events surviving all cuts in the electron, missing energy and jets topology, compared with background expectations, as function of the LQ mass (in  $\text{GeV}/c^2$ ).

Mass	W + 2 jets	top	Z + 2 jets	Total	Data
120	$1.5 \pm 0.9$	$3.3 \pm 0.5$	$0.06 \pm 0.01$	$4.9 \pm 1.0$	6
140	$1.5 \pm 0.9$	$3.1 \pm 0.6$	$0.08 \pm 0.02$	$4.7 \pm 1.0$	4
160	$2.5 \pm 1.1$	$2.8 \pm 0.6$	$0.08 \pm 0.02$	$5.4 \pm 1.2$	4
180	$2.5 \pm 1.1$	$2.4 \pm 0.5$	$0.08 \pm 0.02$	$5.0 \pm 1.2$	4
200	$2.5 \pm 1.1$	$2.0 \pm 0.5$	$0.07 \pm 0.02$	$4.6 \pm 1.2$	4
220	$2.0 \pm 1.0$	$1.6 \pm 0.3$	$0.06 \pm 0.02$	$3.7 \pm 1.1$	2
240	$2.0 \pm 1.0$	$1.1 \pm 0.3$	$0.06 \pm 0.02$	$3.1 \pm 1.0$	2
260	$1.5 \pm 1.0$	$0.8 \pm 0.3$	$0.04 \pm 0.02$	$2.4 \pm 0.9$	2

nal cross section and Gaussian priors for acceptance and background uncertainties. The cross section limits are tabulated in Table I and the mass limits are tabulated in Table III. To compare our experimental results with theoretical expectations, we use the next-to-leading order (NLO) cross-section for scalar leptoquark pair production from Ref.[17] with CTEQ4 PDF[18]. The theoretical uncertainties correspond to the variations from  $M_{LQ}/2$  to  $2M_{LQ}$  of the renormalization scale  $\mu$  used in the calculation. To set a limit on the LQ mass we compare our experimental limit to the theoretical cross section for  $\mu = 2M_{LQ}$ , which is conservative as it corresponds to the lower value of the theoretical cross section. By comparing the 95% CL upper limit on the cross section with the theoretical prediction, we can set a lower limit on the LQ mass. We find lower limits on  $M(LQ)$  at  $235 \text{ GeV}/c^2$  ( $\beta = 1$ ) and  $176 \text{ GeV}/c^2$  ( $\beta = 0.5$ ). To improve our limit however, we have combined the results from the two decay channels just described with the result of a search for leptoquark in the case where the particle decays to neutrino and quark with branching ratio  $\beta' = Br(LQ \rightarrow \nu q) = 1.0$ [8]. A joint likelihood has been formed from the product of the individual channel likelihoods. For each mass we simulated 10K pseudo-experiments, smearing the calculated number of background events and the estimated number of signal events by their respective total uncertainties. The searches in the  $eejj$  and  $e\nu jj$  channel use common criteria and sometimes apply the same kind of requirements so the uncertainties in the acceptances have been considered correlated. When calculating the limit combination including the  $\nu\nu jj$  channel the uncertainties have been considered uncorrelated. For each  $\beta$  value a limit on the expected number of events is returned for each mass. The resulting cross section limit is then compared with the theoretical production cross section to obtain lower limits on the LQ mass. The combined limit as a function of  $\beta$  is shown in Figure 2, together with the individual channel limits. The combined mass limits are also tabulated in Table III. In conclusion, we have performed a search for pair production of scalar leptoquarks in dielectrons +

TABLE III: 95% C.L. lower limits on the first generation scalar leptoquark mass (in  $\text{GeV}/c^2$ ), as a function of  $\beta$ . The limit from CDF[7] ( $eejj$ ) Run I ( $\sim 120\text{pb}^{-1}$ ) is also given.

$\beta$	ee jj	$e\nu jj$	$\nu\nu jj$	Combined	CDF Run I
0.01	-	-	116	126	-
0.05	-	-	112	134	-
0.1	-	144	-	145	-
0.2	-	158	-	163	-
0.3	114	167	-	180	-
0.4	165	174	-	193	-
0.5	183	176	-	205	-
0.6	197	174	-	215	-
0.7	207	167	-	222	-
0.8	216	158	-	227	-
0.9	226	144	-	231	-
1.0	235	-	-	236	213

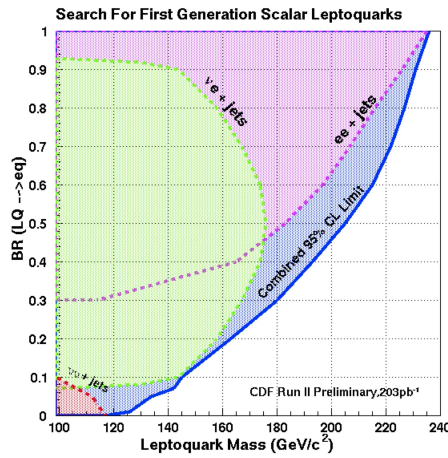


FIG. 2: Leptoquark mass exclusion regions at 95% C.L. as function of  $\text{Br}(\text{LQ} \rightarrow e\text{q})$

jets and electron, missing energy + jets topologies, using  $203\text{ pb}^{-1}$  of proton-antiproton collision data recorded by the CDF experiment during Run II of the Tevatron. We combined these findings with the ones from a search in the  $\cancel{E}_T$  + jets topology[8]. No evidence for leptoquarks is observed. Assuming that a scalar leptoquark decays to electron and quark with variable branching ratio  $\beta$  we exclude leptoquarks with masses below  $236\text{ GeV}/c^2$  for  $\beta = 1$ ,  $205\text{ GeV}/c^2$  for  $\beta = 0.5$  and  $145\text{ GeV}/c^2$  for  $\beta = 0.1$ .

We thank the Fermilab staff and the technical staffs of the participating institutions for their vital contributions. This work was supported by the U.S. Department of Energy and National Science Foundation; the Italian Istituto Nazionale di Fisica Nucleare; the Ministry of Education, Culture, Sports, Science and Technology of Japan; the Natural Sciences and Engineering Research Council of Canada; the National Science Council of the Repub-

lic of China; the Swiss National Science Foundation; the A.P. Sloan Foundation; the Bundesministerium fuer Bildung und Forschung, Germany; the Korean Science and Engineering Foundation and the Korean Research Foundation; the Particle Physics and Astronomy Research Council and the Royal Society, UK; the Russian Foundation for Basic Research; the Comisión Interministerial de Ciencia y Tecnología, Spain; and in part by the European Community's Human Potential Programme under contract HPRN-CT-20002, Probe for New Physics.

- [1] W. Buchmuller, R. Ruckl and D. Wyler, Phys. Lett. B191, 442 (1987) and Erratum B448, 320 (1999).
- [2] D. Acosta and S.K. Blessing, Ann.Rev.Nucl. Part.Sci. **49**, 389 (1999) and reference therein.
- [3] G. Moortgat-Pick, S. Rolli, A.F. Zarnecki, Physics at large  $p(T)^{**2}$  and  $Q^{**2}$ : summary, , Acta Phys. Polon.B33:3955-3981, 2002.
- [4] H1 Collaboration, C. Adloff et al., Eur. Phys. J.C **11**, 447 (1999); Erratum ibid. C **14** 553 (2000); H1 Collaboration, C. Adloff et al., Phys.Lett. B **523**, 234 (2001); ZEUS Collaboration, J. Breitweg et al., Eur. Phys. J.C **16**, 253 (2000); ZEUS Collaboration, J. Breitweg et al., Phys.Rev.D **63**, 052002 (2001).
- [5] DELPHI Collaboration, P. Abreu et al., Phys. Lett. B **446** 62 (1999); L3 Collaboration, M. Acciari et al., Phys. Lett. B **489** 81 (2000); ALEPH Collaboration, R. Barate et al., Eur. Phys. J.C **12**, 183 (2000); OPAL Collaboration, G. Abbiendi et al., Phys. Lett. B **526** 233 (2002).
- [6] D0 Collaboration, V. Abazov et al., Phys. Rev. D **64**, 092004 (2001); D0 Collaboration, hep-ex/0412029; Fermilab-Pub-04/389-E, Dec 2004.
- [7] CDF Collaboration, F. Abe et al., Phys. Rev. Lett. **79**, 4327 (1997).
- [8] CDF Collaboration, D. Acosta et al., hep-ph/0410076, submitted to PRL.
- [9] CDF Collaboration, D. Acosta et al., Fermilab-Pub-04-440-E, 2004.
- [10]  $\eta = -\ln(\text{tg}(\frac{\theta}{2}))$ , where  $\theta$  is the polar angle relative to the proton beam direction.
- [11] M.L. Mangano et al., JHEP **0307**,001 (2003).
- [12] T. Sjostrand et al., High-Energy-Physics Event Generation with PYTHIA 6.1, Comput. Phys. Commun. **135**, 238 (2001).
- [13] R. Brun and F. Carminati, CERN Program Library Long Writup W5013 (1993).
- [14] N. Kidonakis and R. Vogt, Phys.Rev.D **68**, 114014 (2003).
- [15] M. Cacciari et al., JHEP **404**, 68 (2004).
- [15] J. Campbell, R.K. Ellis and D. Rainwater, Phys.Rev.D **68**, 094021 (2003).
- [16] J. Conway, CERN 2000-005, 247 (2000). The posterior probability density is rendered normalizable by introducing a reasonably large cutoff.
- [17] M. Kramer et al., Phys Rev Lett **79**, 341, 1997.
- [18] J. Pumplin et al., JHEP **0207** (2002) 012.